Next-Generation X-ray Free-Electron Lasers*

Alexander Zholents, *Advanced Photon Source, Argonne National Laboratory, Argonne, IL 60439*

***Abstract*— Research frontiers for future free-electron lasers are discussed. Attention is given to ideas for improving the temporal coherence and obtaining sub-femtosecond x-ray pulses. Improving brightness of the electron bunches is considered to be a major step forward for an electron beam accelerator simultaneously supporting multiple free-electron laser lines.**

***Index Terms*—Attosecond, brightness, EEHG, electron gun, emittance, HGHG, FEL, femtosecond, linac, oscillator, SASE, self-seeding, XFELO, x-rays.**

I. Introduction

A free-electron laser (FEL) facility consist of two major components: the FEL itself that contains a chain of undulator magnets plus auxiliary equipment, and the electron beam delivery system that includes the electron gun, linear accelerator, laser heater, and bunch compressors. Major advances have been made in both areas that have helped bring to life x-ray FELs. This process continues to evolve, and new ideas continue to germinate and take root. Here we review some of the ideas that seem to be within the reach without requiring a breakthrough in technology. In the first part we describe some possible scenarios for future development of the FELs, and in the second part we describe possible improvements in the electron beam delivery system.

II. Free-electron lasers

Recent commission of the LCLS [1], the hard x-ray FEL, completed a several-decades-long quest for an x-ray laser and culminated the emergence of the 4th-generation light sources or the first generation of x-ray FELs. The LCLS joined a small family of two existing extreme ultraviolet (EUV) FEL facilities, i.e., FLASH [2] and SCSS [3]. Two new hard x-ray FEL facilities, i.e., European XFEL [4] and Japanese XFEL [5], are currently under construction. There are plans to build two additional hard x-ray FELs, i.e., Swiss XFEL [6] and Korean XFEL [7], and to add new FELs to FLASH [8] and LCLS [9] as an upgrade. All these FELs employ a process of self-amplified spontaneous emission (SASE) [10, 11] to obtain an intense, spatially coherent, and partially temporally coherent light with peak brightness more than ten orders of magnitude larger than the peak brightness of third-generation storage-ring-based light sources [12]. The entire history of the development of the first generation of x-ray FELs is documented in several review articles (see, for example, [12-18]) and numerous research papers [19], reflecting a growing understanding of the underlying physics, the development of numerical simulation tools, and a steady progress in the accelerator technology, most notably in the production and preservation of high-brightness electron beams.

Although it will take some time to complete all construction projects and also to fully explore new capabilities provided by the first generation of x-ray FELs, there is a growing interest in the scientific community to define what should come next. At least one goal has been known for quite a long time. This is obtaining a laser-like x-ray beam with temporal coherence by "seeding" the FEL amplifier with an external temporally coherent signal [20-23]. Seeded FELs employing the process of high gain harmonic generation (HGHG) [23,24] use a laser for energy modulation of electrons in the first undulator; convert it into density modulation using a magnetic chicane, with the result of obtaining a relatively large microbunching of electrons at a high harmonic n of a laser frequency; and produce amplified radiation in the downstream undulator tuned on the FEL resonance [25] at harmonic frequency. This technique has been proposed as a marked improvement to SASE FELs, capable of laser-like x-rays with a time-bandwidth product approaching a Fourier transform limit. A proof-of-principle experiment [26] has demonstrated a substantial increase of spectral brightness in an HGHG FEL compared to a SASE FEL and much better wavelength stability. Typically, the harmonic number is limited to less than five because of debunching caused by the incoherent energy spread of electrons $b \sim e^{-(n\sigma_E/\Delta E)^2}$, where b is the bunching factor, and ΔE is the amplitude of the energy modulation. Thus, further extension of the HGHG technique to reach short-wavelength x-ray radiation consists of adding two or more cascades. In this case, a fresh part of the electron bunch can be used in each cascade [23,24,26]. The first FEL to be built with more than one cascade will likely be the FERMI@elettra FEL [27], which is currently going through its final phase of commissioning.

The processes of high harmonic generation (HHG) in rare gases [28] and solids [29] are also considered as sources of a Fourier-transform-limited seed signal. In this case, the FEL just amplifies a seed if it is already at a requisite frequency [30] or uses it in the same way as the laser seed in HGHG [31]. In the first case, the power of the HHG seed signal in the undulator must be substantially larger than a shot noise power of electrons within the bandwidth of the seed signal $P_{Noise} \approx \pi\alpha\hbar\omega I/e \times (\ell_c/c\tau_L)$, where α is a fine structure

* To be published in Journal of Selected Topics in Quantum Electronics.

constant, $\hbar$ is Plank's constant, e is the electron charge, c is the speed of light, ω is a seed frequency, I is the electron peak current, ℓ_c is the temporal coherence length of the FEL produced signal, and τ_L is the seed signal pulse width, or in the second case, it must be large enough (e.g., often at a few megawatt level) to be able to produce ΔE at least n times larger than σ_E. FLASH FEL has been recently modified to include the HHG seeding as a new mode of operation [8], which is currently undergoing the final phase of commissioning.

However, future x-ray FELs will most likely use another seeding technique called echo- enabled harmonic generation (EEHG) [32] because of its superior efficiency in creating the microbunching at high harmonics when the bunching factor only weakly decreases with the harmonic number, i.e., $b \sim n^{-1/3}\Delta E/\sigma_E$ [32]. All details of EEHG can be found in Ref. [33,34]. Here we want only to emphasize that EEHG reduces the complexity of a multi-staged HGHG FEL and eradicates a need in HHG due to its capability for microbunching at the wavelengths reachable with HHG and even shorter. Moreover, EEHG can be combined with HGHG in order to produce light at an even higher harmonic than EEHG can do alone; however, it remains to be seen how far into the x-ray range one can go using EEHG or EEHG plus HGHG seeding. One known obstacle is the spontaneous emission in the two sets of chicane magnets employed in the EEHG that causes a mix up of the electrons in the longitudinal phase space. However, most of the beam manipulations needed for EEHG can be done at a relatively low energy where spontaneous emission is weak. Another potential problem that is common for all seeding methods is caused by the amplitude and phase noise of the seed laser [35]. This noise affects temporal coherence of the light produced in the FEL at high harmonics of the seed laser. The higher the harmonic number, the stronger the impact of the noise. Thus, extending seeding methods into a hard x-ray range seems to be problematic. Fortunately, this may not even be needed thanks to the idea of self-seeding [36], which is best suited for hard x-rays where crystal monochromators can be used [37].

The FEL self-seeding technique does not rely on an external laser, but rather utilizes undulator x-ray output generated from the electron bunch itself, which is monochromatized to ensure temporal coherence and then made to overlap the same electron bunch, suitably delayed. The simplest approach for the self-seeding is called a wake monochromator [38], shown in Fig. 1. The entire scheme consists of the SASE FEL (the left part in Fig. 1), the insert with the weak magnetic chicane and the diamond crystal (the middle part), and the FEL amplifier (the right part). The SASE FEL operates in the high-gain regime starting from the shot-noise in the electron beam. Its output radiation passes through a thin diamond crystal that acts as a bandstop filter in Bragg transmission geometry. Because of the Bragg reflection, the spectrum of the transmitted light exhibits an absorption line with a narrow width. After such filter, the waveform of the transmitted light acquires a relatively long monochromatic part behind the main pulse, called the wake in the original proposal. The amplitude of this wake is much smaller than the amplitude of the main pulse, but is still large enough to be used for seeding the FEL amplifier. The magnetic chicane accomplishes three tasks: it creates an offset for crystal installation; it removes the electron microbunching produced in the SASE FEL; and it acts as a delay line for the electron bunch, matching its arrival time in the downstream undulator with the arrival time of the wake. The amplified signal reaches 10 – 100 GW peak power level and has approximately 10^{-5} relative bandwidth. Since this scheme starts with a SASE FEL, it is expected to have large pulse-to-pulse fluctuations of the intensity in the output signal due to fluctuations in the spectrum of the radiation incident on the diamond crystal.

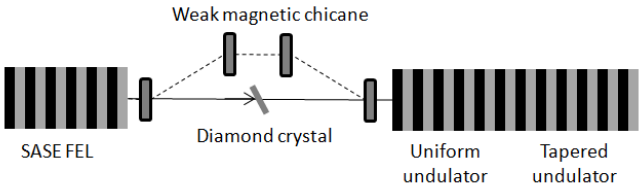

Fig. 1. The proposed self-seeding system as described in Ref. [38].

Another approach to produce temporal coherent light, proposed in [39, 40], also falls under the category of a self-seeding FEL although it actually uses two electron bunches. A schematic of this approach is shown in Fig. 2.

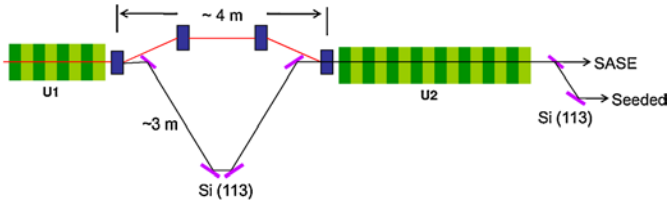

Fig. 2. (color online) Schematic of the two-bunch self-seeding layout as described in Ref.[40]. The total path length delay introduced by the two-crystal monochromator is about 3 m (10 ns), matching the distance between two bunches (not shown).

Here the spectrally filtered SASE light produced by the first bunch in U1 is combined with the second bunch at the entrance of the FEL amplifier U2 where it is amplified to the saturation level. The time delay for the x-ray pulse between U1 and U2 is provided by the V-shaped zigzag in the light path and the two-crystal monochromator. It can be precisely tuned to match the separation of the two electron bunches with any convenient spacing. The electron beam chicane serves two purposes. It creates electron beam offset to give space to the x-ray optics and it provides smearing of the Angstrom-scale microbunching of the electron beam. All that can be accomplished with a small orbit offset using rather modest magnets. The peak power calculated for LCLS is approximately 10 GW and the relative bandwidth is approximately 10^{-5}. A set of two crystals at the end of the FEL

amplifier assists in separating the seeded signal from the SASE signal.

While self-seeding methods are very attractive for hard x-ray FELs, for soft x-rays they seem to be less important due to the enormous advantages of external seeding techniques offering exquisite control over x-ray pulses needed for high-precision, time-resolved pump-probe or other experiments. A completely different approach to achieve temporal coherence is to use an FEL in an oscillator configuration. The principles of an FEL oscillator are well known [41]. A light pulse trapped in an optical cavity and an electron bunch from an accelerator meet at the entrance of an undulator and travel together. The amplified light pulse at the end of the undulator is reflected back to the entrance where it meets a fresh electron bunch, and so on. The light pulse evolves from initially incoherent spontaneous emission to a temporal coherent pulse as its intensity rises exponentially until saturation is achieved. The idea to build a tunable hard x-ray FEL oscillator was first proposed more than 25 years ago in [42], but began to gain a momentum only recently [43-46] after an ultra-low emittance electron beam with a peak current sufficient to support low-gain amplification in the oscillator configuration became feasible. An oscillator configuration, shown in Fig. 3, was put forth in [43] using a realizable set of electron beam parameters and narrow-bandwidth diamond crystals with more than 95% reflectivity in the Bragg reflection geometry [45]. X-ray tunability is achieved by changing the x-ray incident angle on the crystals while simultaneously adjusting the crystals' relative positions and preserving the roundtrip time over the resonator cavity matching a MHz repetition rate of the electron bunches. As shown in [44], the x-ray FEL oscillator can produce fully coherent x-ray pulses with megawatts of peak power, a relative bandwidth of 10^{-7}, and an average spectral brightness on the order of 10^{26} photons/sec/(mm-mrad)^2/0.1%BW.

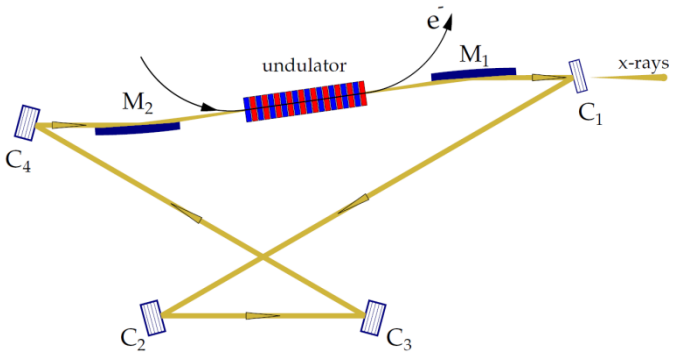

Fig. 3. (color online) Schematic of a hard x-ray FEL oscillator as shown in Ref. [44]. The electron beam path into and out of the undulator is indicated with arrows.

Various FEL oscillator ideas were investigated in the past for the EUV range of photon energies [47-51]. While a diamond crystal reflector works with high efficiency for hard x-ray photons, this mirror technology cannot be used for soft x-ray photons. The other technology of choice is multilayer mirrors with a reflectivity of 50%-70% available at several discrete wavelengths between 13 nm and 70 nm [52]. Taking advantage of this technology and the EEHG seeding technique discussed above, a tunable soft x-ray FEL was proposed in [53] that is largely based on the oscillator idea. Figure 4 shows a schematic of this concept. The system consists of a progression of two FEL oscillators and an FEL amplifier. In a particular example considered in [53], the first oscillator operates at 43-nm wavelength using two multilayer mirrors with a backward reflectivity of 70%. The second oscillator operates at a 215-nm wavelength and uses conventional UV mirrors. The purpose of the first oscillator cavity is to energy modulate the electron bunch and simultaneously produce a partial microbunching of electrons such that they radiate the light with just enough intensity to overcome mirror losses and are capable of inducing energy modulation at 43-nm wavelength with the required amplitude. The light power in the cavity need not be high, thus helping to run it with a relatively modest heat load on the mirrors. The second oscillator practically serves all the same purposes, but does it at 215 nm. The first chicane moves the electron beam out of the first oscillator and brings it into the second oscillator. At the same time it provides stretching of the energy-modulated electrons in the longitudinal phase space, as required by the EEHG process. The second chicane takes the electron bunch out of the second oscillator and prepares a seed microbunching for a downstream FEL amplifier according to the EEHG process at a high harmonic number of 215-nm wavelength. The electron bunch repetition rate is 1 MHz. The x-ray wavelength tunability is achieved by a slight modification of the time-of-flight parameters of both chicanes that shifts the seed microbunching from one harmonic to the other harmonic. Of course, the FEL amplifier is also tuned in accordance with the change of the harmonic. We note that the FEL amplifier can be tuned rather continuously thanks to relatively broad harmonic peaks in the EEHG-induced microbunching.

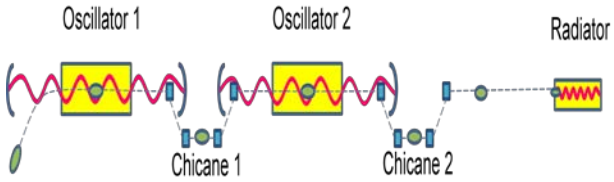

Fig. 4. (color online) A concept of the soft x-ray FEL oscillator as shown in Ref. [53].

The FEL is a naturally "born" source of ultra-short x-ray pulses and can be used in conjunction with a conventional laser, producing femtosecond optical pulses for pump-probe studies of matter with femtosecond resolution. However, the capabilities of existing SASE FELs are rather underused because of a jitter in the electron bunch arrival time in the FEL. The situation can be significantly improved by using an external laser linked to a pump source to affect lasing in the FEL. Possible implementation of this approach is shown in Fig. 5 (see also, [54]).

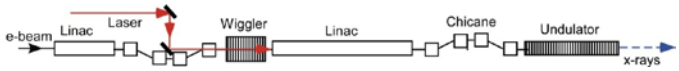

Fig. 5. (color online) Schematic of a current enhanced SASE x-ray FEL as shown in Ref. [54].

Here the electron bunch arriving from the first part of the linac enters a wiggler magnet. At the same time a short laser pulse (shorter than the electron bunch minus a jitter in the arrival time of the electron bunch) enters the wiggler and co-propagates it with the electrons. The laser pulse overlaps only a short section of the electron bunch, whose arrival time in the wiggler corresponds to the arrival time of the laser pulse. For convenience we call this section of the electron beam the working section (WS). Electrons in the WS interact with the laser field and emerge from the wiggler with an energy modulation. The laser pulse energy is chosen such that the amplitude of the energy modulation exceeds the uncorrelated energy spread of the electrons by a factor of 5 to 10. Next, the electron beam enters a second linear accelerator and gains energy to reach the final energy. This acceleration does not affect the energy modulation introduced in the wiggler and does not produce noticeable relative longitudinal motion of electrons because of the ultra-relativistic electron energies. Following acceleration, the electron beam passes through a dispersive magnetic chicane that produces micro-bunching of the electrons in the WS and periodic enhancement of the electron peak current. Finally, the electron beam passes through a long undulator where electrons inside the WS produce enhanced SASE (ESASE) because of the current enhancement. The x-ray radiation produced by electrons outside of the WS has significantly less intensity because of the longer gain length at a significantly lower peak current. Thus, there is precise synchronization between the output x-ray pulse and the laser pulse since only electrons from the WS, i.e., the region that experienced interaction with the laser, produce intense x-rays. Moreover, by changing the duration of the laser pulse and adjusting the number of active wiggler periods, one can regulate the length of the WS and therefore the duration of the x-ray output. It is beneficial to have the same laser producing two laser pulses: one for energy modulation of electrons and one as a pump source. Fortunately, it is also possible to determine the relative timing between laser pump pulse and x-ray probe pulse at the end of the FEL. Besides generating powerful x-rays, electrons from the WS can produce strong coherent synchrotron radiation at the modulating laser frequency (which is automatically temporally synchronized with the x-ray pulse) in one period wiggler that can be placed at the end of the FEL. This signal can be cross-correlated with the laser pulse to provide an accurate measure of the remaining time jitter between the laser pump pulse and the x-ray probe pulse. We also note that if a wiggler is not available, perhaps either edge radiation from the bending magnet turning the electron beam into the dump or transition radiation from the thin foil can be used.

Remarkably, the seeded FELs discussed above naturally possess a precise synchronization between laser and x-ray pulses, as they are linked to each other through laser electron beam interaction that eventually leads to generation of x-rays. Similar to the current enhanced SASE technique, changing the duration of the seed laser pulse directly affects the duration of the x-ray output.

To date, a few femtoseconds-long x-ray pulses have been obtained [55] using FELs and several ideas have been proposed (see, [56] and references therein) on how to make even shorter pulses down to sub-femtosecond duration using seed laser pulses with only a few optical cycles and carrier-envelope phase (CEP) stabilization [57-59]. Such a laser pulse interacting with the electrons in the wiggler magnet with just one or two periods produces energy modulation of electrons with a waveform that closely resembles the waveform of the laser electric field. For example, manipulating the carrier-envelope phase, one can obtain a cosine-like waveform of the energy modulation when the peak of the electric field is at the maximum of the envelope or a sine-like waveform when a zero crossing of the electric field is at the maximum of the envelope (see Fig. 6).

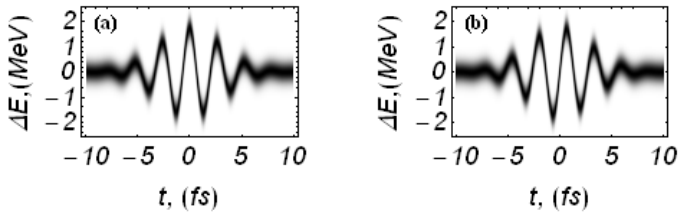

Fig. 6. Density plot showing energy modulation of electrons produced in the interaction with a few-cycle, 800-nm-wavelength laser pulse with CEP stabilization interacting with the electron bunch in the wiggler magnet with two periods. Only a small fragment of the electron bunch longitudinal phase space cut at ± 10 fs points along the electron bunch is shown. (a) A cosine-like form, and (b) a sine-like form.

As an illustration, we consider here the proposal [60] that uses a strong, temporally localized energy chirp $d\gamma/dt$ (i.e., the variation of the electron energy with the time) in the center of the sine-like modulation waveform shown in Fig. 6(b). Under normal conditions the energy chirp causes the FEL gain degradation, but it can be prevented by means of the undulator tapering producing z dependence of the undulator parameter K. It can be understood by considering that the field experienced by the test electron was emitted by a second electron behind it at a retarded time. It is best when the carrier frequency of this field is in the FEL resonance with the test electron, e.g., when $\gamma^2 = \lambda_u / 2\lambda_S \times (1 + K^2/2)$, where λ_u is the undulator period, and λ_s is the wavelength of the field. Therefore, the second electron with the energy offset can only emit the field with the right frequency if undulator parameters are different at the retarded time. For large $d\gamma/dt$ this requirement can be formulated with an approximate condition: $d\gamma/cdt \times (\bar{\beta}_z - 1) \approx (d\gamma/dK) \times (dK/dz)$, where β_z is the electron longitudinal velocity averaged over the undulator

period and normalized on *c*. Equivalently, one can obtain [60,61]:

$$\frac{d\ln K}{dz} = -\frac{\lambda_s}{\lambda_u}\frac{1+K^2/2}{K^2/2}\frac{d\ln\gamma}{cdt}.$$

With the above-defined undulator taper, only a short slice of the electron bunch around the zero-crossing of the energy modulation in Fig. 6(b) will produce a powerful FEL pulse. The main unmodulated part of the electron bunch will suffer from the undulator taper and will have much reduced or nonexistent FEL gain. Figure 7 shows that, in fact, the calculated output signal is dominated only by one slice of the electron bunch. Typical pulse duration of the peak is about 200 attoseconds (FWHM), and typical peak power ranges up to 100 GW. The estimated total number of photons in the collimated attosecond pulse is about the same as the total number of photons in two side peaks (barely visible in Fig. 7) plus all photons produced by spontaneous and SASE emission from the rest of the electrons [60].

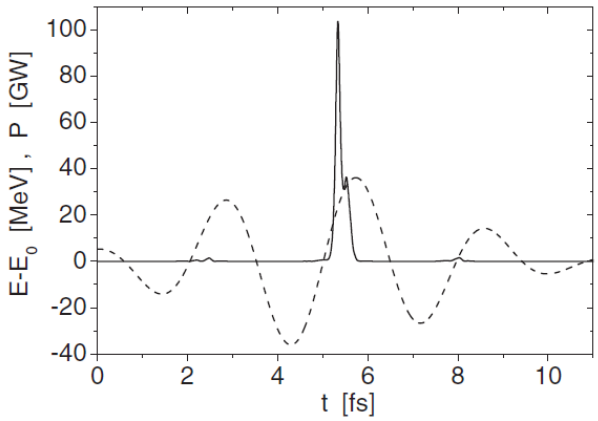

Fig. 7. Energy modulation of the electron beam at the exit of the modulator undulator (dotted line), and a profile of the radiation pulse at the exit of the FEL (solid line) as shown in Ref.[60].

Besides experiments using optical pump and x-ray probe pulses, there is a growing interest in the user community for studies of the ultra-fast dynamics using two-color x-ray pump and x-ray probe pulses [62,63]. This is not an easy task for a typical FEL, but recently some ideas have started to form. One possibility [64], exploring EEHG seeding techniques, is schematically shown in Fig. 8.

The beginning of this scheme is the same as the EEHG seeding technique, e.g., the electron bunch is energy-modulated in wiggler W1 and then sent through a dispersion section C1, after which the modulation obtained in W1 produces separated energy bands in the longitudinal phase space. Then the following part aims for production of two-color, two attosecond x-ray pulses with a well-controlled time delay. In wiggler W2 a few-cycle laser pulse interacts with a short WS of the electron bunch and produces a sine-like form of energy modulation with carefully adjusted amplitude. Then, on the basis of this modulation, the following dispersion section C2 enhances the peak current as in the ESASE technique and converts energy bands within a narrow slice of the WS located in the vicinity of a zero-crossing of the energy modulation waveform into the modulation of the peak current and hence produces microbunching. The magnitude of the dispersion in C2 is carefully chosen such that the energy modulation in M2 can be utilized to yield the microbunching at a specific x-ray wavelength λ_{x1}. Then electrons bunched at λ_{x1} produce an attosecond pulse of coherent radiation in the downstream undulator R1. The entire process between M2

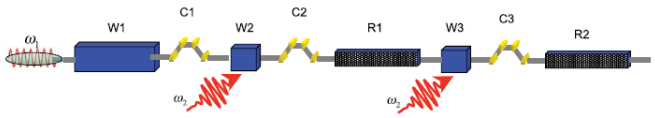

Fig. 8. (color online) Schematic of the generation of two attosecond x-ray pulses, where W1, W2, and W3 are wiggler magnets; C1, C2, and C3 are dispersion sections; R1 and R2 are x-ray undulator radiators; ω_1 is the carrier frequency of the long laser pulse; and ω_2 is the carrier frequency of a few-cycle laser pulse that is split into two pulses [64].

and R1 is then repeated using a new few-cycle laser pulse and a new short WS of the electron bunch, but this time the amplitude of energy modulation in M3 and the magnitude of the dispersion in C3 are adjusted to yield the microbunching and attosecond pulse in the undulator R2 at a different x-ray wavelength λ_{x2}. Since both few-cycle laser pulses can be originated from the same source, the time delay between two laser interactions with the electron bunch in M2 and M3 can be precisely adjusted to yield ultimate control over the time

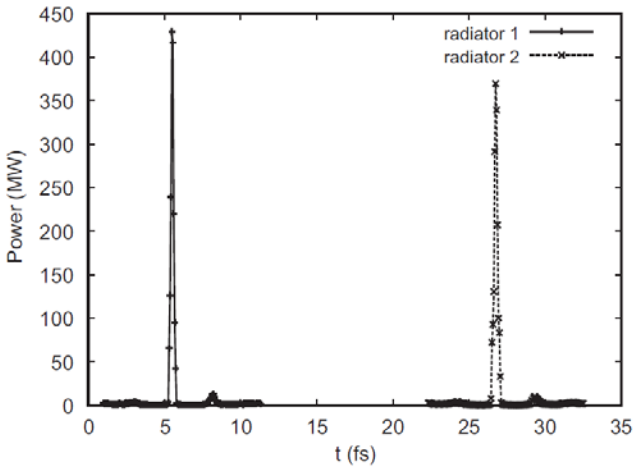

Fig. 9. Two x-ray pulses produced in undulators R1 and R2. Coherent radiation of the bunched electrons dominates spontaneous emission as shown in Ref.[64].

delay between two attosecond x-ray pulses. Moreover, the relative phase of the electric field oscillations in these pulses can also be controlled and well defined. The time delay between two attosecond x-ray pulses can vary from a few fs to a hundred of fs, being limited only by the width of the electron bunch length minus timing jitter in the arrival time of the

electron bunch in M2. Figure 9 shows computer simulation results for the above-described scheme wherein the frequency of the first attosecond pulses is tuned to the oxygen K-edge and the frequency of the second attosecond pulses is tuned to the nitrogen K-edge. The FWHM length of both pulses is ~200-250 attoseconds and the FWHM bandwidth is ~6-8 eV. We note that the relative phase of the electric field oscillations in both pulses is locked to each other because they have the same original source for few-cycle laser pulses in W2 and W3.

Perhaps the most straightforward way to obtain two x-ray pulses with two different photon energies from the same electron bunch is to use two FELs in line one after another. They can be positioned at a slight angle provided by an achromatic bend that can also be used to remove microbunching of electrons induced in the upstream FEL. The first FEL will operate with a higher photon energy, meeting a stringent requirement for the electron beam energy spread, and the downstream FEL will operate with lower photon energy, accommodating an electron beam with degraded energy spread. A number of ideas for a practical realization of the concept of two FELs have been already proposed [9,65,66] including some for existing FELs (i.e., see [67]). There are actually many more ways to combine two FELs that may also include using more than one electron bunch and generation of THz and infrared pulses at the end of the FELs for pump-probe experiments using electron bunches coming out of the FEL [65,68].

For reader convenience all FEL schemes discussed above are briefly summarized in Table 1 and Table 2.

Table 1. List of the FEL schemes capable of producing x-ray pulse with a temporal coherence.

Scheme	Technique	Number of e-bunches per x-ray pulse	Number of FELs	Relative bandwidth	Applicable to:
EEHG	external seeding	1	two modulators, one FEL	defined by the bunch length, 10^{-4} - 10^{-5}	soft x-rays
Fig.1	self-seeding	1	2	~ 10^{-5}	hard x-rays
Fig.2	self-seeding	2	2	10^{-4}-10^{-5}	soft/hard x-rays
Fig.3	FEL oscillator	1	1	defined by the bunch length, ~ 10^{-7}	hard x-rays
Fig.4	EEHG using two FEL oscillators	1	1	defined by the bunch length, 10^{-5} - 10^{-6}	soft x-rays

Table 2. List of the FEL schemes capable of producing ultra-short x-ray pulses.

Scheme	Technique	Synchronization to external laser with CEP	Number of x-ray pulses per e-bunch	Pulse duration	Applicable to:
Fig.5	ESASE	yes	1	defined by the laser, 10-th fs to 100-th as*	hard x-rays
Fig.7	chirped e-bunch and tapered undulator	yes	1	few fs (soft x-ray) 100-th as (hard x-ray)	soft/hard x-rays
Fig.8	EEHG	yes	two pulses of two color	~ 200 as	soft x-rays

* Here "as" stands for attoseconds.

III. ELECTRON BEAM DELIVERY SYSTEM

The brightness of the electron beam $B_n = (N_e \lambda_c)/(\varepsilon_x \varepsilon_y \varepsilon_z)$, where N_e is the number of electrons in the electron bunch; $\varepsilon_x \varepsilon_y \varepsilon_z$ are the normalized horizontal, vertical, and longitudinal emittances; and $\lambda_c \approx 3.86 \times 10^{-11}$ cm is Compton wavelength, plays the most important role in the FEL process. It was shown in [69,70] that in the best possible scenario when electron beam and FEL parameters are optimized to yield the fastest growth rate of the micro-bunching, the inverse gain length in the FEL scales linearly with brightness and quadratically with the electron beam energy (a typo in [69] shows a linear dependence), i.e.,

$$\frac{\lambda_u}{L_g} \propto \frac{K^2}{2+K^2}\left(\frac{E_b}{\hbar\omega_s}\right)^2 B_n \ , \qquad (1)$$

where L_g is the gain length, $\hbar\omega_s$ is the x-ray photon energy, and E_b is the electron beam energy.

The electron beam energy is the next most important parameter after brightness that strongly affects the FEL performance. Besides Eq. (1), E_b appears in the optimization of FEL performance in a few other places. The first one is a constraint on the geometrical emittance $\varepsilon_{x,y} / \gamma \le \lambda_s / 4\pi$, providing that the electron beam size matches the light beam and electrons do not de-phase over the FEL gain length due to betatron oscillations. The second is a constraint on the relative energy spread σ_E/E_b, which is basically driven by the same de-phasing concern. The third one is the FEL resonance condition $\lambda_s = \lambda_u / 2\gamma^2 \times (1 + K^2/2)$. At last, the electron beam energy almost solely defines the cost of the electron beam delivery system. Thus, according to these listed constrains, the next-generation FELs should rely on increased brightness of the electron beam and undulators with short periods in order to lower E_b and, thus, the cost of the FEL.

Undulator performance is characterized by the peak magnetic field on the undulator axis as a function of a given beam-stay-clear aperture (gap) g inside the vacuum chamber and undulator period λ_u. Evidently, the smaller the gap, the higher the field. Figure 10 shows a comparison of several existing technologies, i.e., pure permanent magnet (PM) in-vacuum devices with a remanence field of 1.35 T, hybrid PM in-vacuum devices with steel poles, superconducting helical devices using low-temperature superconducting wires, and a new emerging technology where the undulator is made out of stacks of high-temperature superconducting YBCO ($YBa_2Cu_3O_7$) tapes [71]. Different technologies excel in different regimes with respect to g and λ_u, and a comparison is provided for 5 mm < λ_u < 10 mm and g = 2 mm.

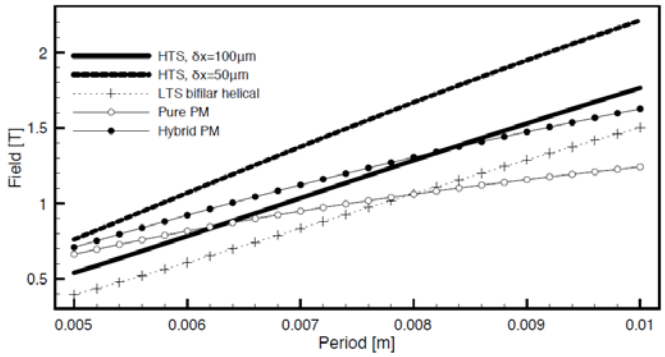

Fig. 10. Peak magnetic field in the undulator as a function of the undulator period calculated for several undulator technologies [71]. In the case of HTS tapes, a stack of 25 tapes was assumed in the calculations. A 100-μm tape is a standard commercial product and a 50-μm tape can be readily obtained by eliminating the stabilizer material.

One can see that permanent magnet devices perform rather well at short λ_u. However, their fabrication is labor intensive, requiring precise machining, assembly, and shimming of magnetic poles, and these issues become more severe as λ_u decreases. On the other hand, the high-temperature superconducting (HTS) devices described in [71] dominate the entire range. Such performance combined with a potentially uncomplicated machining and assembly makes them the most favorable candidates for the next generation of FELs possessing shorter and more cost-effective undulator lines. A few other approaches to building short-period undulators are described in [72-75]. As expected, all these concepts rely on small g, and the concern is that it increases wakefields produced by the electron bunch travelling inside a narrow-gap vacuum chamber. Thus, it is planned to offset the energy chirp caused by the wakefields by using pre-chirped bunches and tapered undulators and/or reduce wakefields by using electron bunches with lower charge.

Lowering the charge of electron bunches can also help obtaining higher brightness beams. This trend has been observed at LCLS [55] and was predicted in [76]. It was also used as a strong argument in favor of FELs operating with ultra-low-charge bunches of the order of 1 pC [77]. The brightness is largely defined by the ability of the electron gun to produce a small emittance, and the ultimate brightness obtainable with low-charge bunches is defined by a so-called intrinsic emittance (IE), which is solely dependent on the cathode material work function φ_0 and an electron extraction mechanism. For example, measurements of the IE in the case of the photoemission from a Cu cathode shown in Fig. 11 [78] demonstrate that it depends on the difference between photon energy $\hbar\omega$ and the effective work function $\varphi_{eff} = \varphi_0 - (e^3 E_c)^{1/2}$ (in CGS untis),

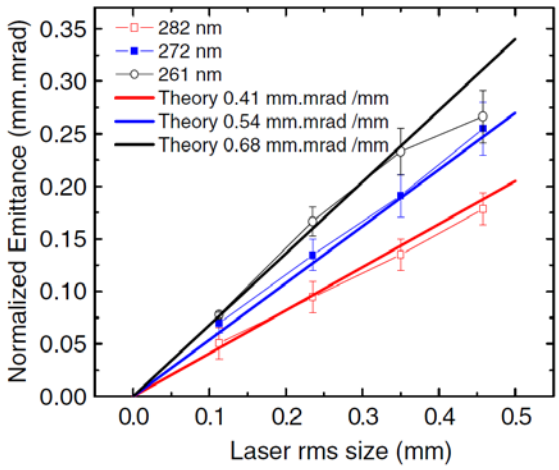

Fig. 11. (color online) Normalized projected emittance versus laser spot size for three different laser wave lengths as shown in Ref.[78]. Measurements were carried out for copper cathode using a low charge less than 1 pC and E_c=25 MV/m. Theoretical fit assumes φ_0 = 4.3 eV. Thermal effects are not included.

where e is the electron charge, and E_c is the applied electric field on the cathode surface responsible for

reduction of the potential barrier due to the work function φ_0. Here one can see that the smaller the excess energy $\hbar\omega - \varphi_{eff}$, the smaller the IE [79]:

$$\varepsilon_{\text{intrinsic}} = \sigma_r \sqrt{\frac{\hbar\omega - \varphi_{eff}}{3mc^2}} \ , \qquad (2)$$

where σ_r is the rms size of the laser beam on the cathode, and *m* is the electron mass. This trend was also observed with Mo, Nb, Al, and bronze cathodes [78] and is expected in semiconductor cathodes such as Cs_2Te and SbK_2Cs [80]. Thus, matching the work function of the cathode material to laser photon energy is expected to yield better IE.

In theory, the quantum efficiency (QE) of the cathode, i.e., the number of extracted electrons per incident photon, is directly connected to excess energy. A drop in QE is expected when one approaches the limit where the photon energy barely exceeds the effective work function. However, for small charge bunches, the drop in QE can be compensated with a more powerful laser, and for future x-ray FELs this could be a viable approach to an ultimately small emittance and, thus, ultimately bright beams.

Other effects such as surface roughness, electron-electron scattering near the cathode surface, and non-uniformity of electron emissivity over the cathode surface could also affect IE. Cathode contamination and lifetime are also important issues for a light source operating nonstop for long periods of time. Besides aiming for more robust cathodes, the current approach for overcoming adverse

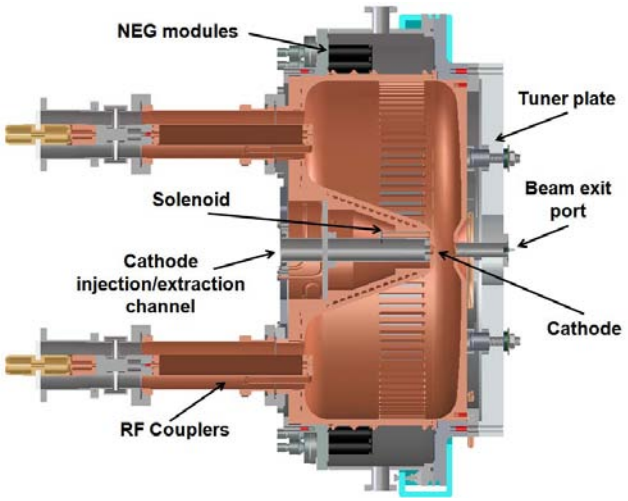

Fig. 12. (color online) The VHF electron gun cavity showing main components and NEG pumping modules shown in Ref. [82].

effects consists of improving the vacuum. A promising design has been proposed in [81,82], where a VHF rf gun is projected to achieve low 10^{-11} Torr vacuum while holding a relatively high E_c =20 MV/m in a continuous wave (cw) operation (see Fig. 12). Assisting in achieving high vacuum are numerous high-conductance vacuum ports seen on the periphery of the central part of the cavity coupled to a pumping plenum containing non-evaporating getter (NEG) modules.

According to Liouville's theorem, in an ideal case, the normalized brightness of an electron bunch is invariant along the electron beamline, but in reality, its conservation can only occur with carefully considered design of the electron beam delivery system. A good example of this practice is the LCLS linac equipped with a laser heater [83], two bunch compressors [84,85], and a beam transport line where the normalized slice emittance remains practically unchanged over the entire process of the electron bunch acceleration and compression, resulting in an increase of the electron peak current from a few tens of amperes in the injector to up to a few kiloamperes at the end of the linac. Similar attention to all details of the beam delivery system, including field quality of magnetic elements, precision alignment of all magnetic elements and linac modules, transverse and longitudinal wakefields, coherent synchrotron radiation, intrabeam scattering, transverse and longitudinal space charge effects, microbunching instability, and diagnostics and feedback systems should be expected in the next generation of x-ray FELs. Obviously, the impact of all collective effects can be greatly reduced by using lower-charge bunches. Additionally, the uncorrelated energy spread that is artificially increased in the LCLS by the laser heater to suppress the microbunching instability in intense bunches can be reduced for low-charge bunches, resulting in more brighter beams.

Evidently, a lower-charge bunch gives less photons. Increasing bunch repetition rate will help to compensate this loss and boost the total number of photons integrated over the same period of time. However, normal-conducting linacs are quite limited in repetition rate under realistic operating conditions and pragmatically only superconducting rf (SRF) linacs can support high bunch repetition rate. Currently, an accelerating gradient over 20 MV/m can be reliably achieved in SRF in cw operation, but a lower gradient may be preferred when full construction and operating costs are considered. Aiming for future applications in the x-ray FELs, current R&D is focused on increasing the Q-factor of cavities at a 25 MV/m gradient. Promising results have been obtained using atomic layer deposition (ALD), where it seems possible to control the surface composition of niobium SRF cavities, control multipactoring, improve the Q-factor, and synthesize superconducting structures with a significantly improved critical field [86,87]. It is then assumed that multiple FEL lines will be simultaneously supported by a single SRF linac [88,89], providing uniformly spaced electron bunches at a few-MHz repetition rate. The same high-repetition-rate performance is expected from the electron gun and various scenarios are currently being considered including a DC gun [90], a superconducting gun [91], and a normal-conducting VHF gun, briefly described above.

IV. CONCLUSION

Promising innovations in FEL technology were discussed. The focus was on new proposals to allow high temporal coherence of the x-ray pulses in addition to a full transverse coherence, a highly anticipated step toward realizing a true laser-like x-ray source. Briefly mentioned were several seeding options for soft x-ray FELs, two self-seeding options for hard x-ray FELs, and one hard and one soft x-ray FEL oscillator. All these techniques are capable to a high degree of temporal coherence with seeded FELs also offering high-precision synchronization of the x-ray pulses to external laser sources for pump-probe experiments. Another possibility for a precision synchronization to an external laser was the briefly mentioned technique of current-enhanced self-amplified spontaneous emission. Generation of sub-femtosecond x-ray pulses was considered, and the feasibility of this principle was demonstrated by two examples: one with a solitary hard x-ray pulse, and one with two-color, two soft x-ray pulses with a variable time delay between them. The electron beam delivery system was considered as an integral part of all FELs, and the importance of high-brightness beams was highlighted. A trade-off of high-charge bunches for high-brightness bunches was favored and the need and opportunities for electron guns providing low-electron-beam emittance was discussed. Finally, a next-generation FEL user facility with multiple FEL lines simultaneously supported by a single accelerator was envisioned. Outside of the scope of this paper were the more radical ideas of plasma-based undulators [92,93], "laser undulators" [94-97,69], and novel acceleration methods exploring plasma wakefields [98]. A longer time to maturity was presumed for all of these ideas

ACKNOWLEDGMENT

I gratefully acknowledge that during the many years I had the pleasure to discuss various aspects of free-electron lasers and electron beams with many people including S. Chattopadhyay, M. Cornacchia, S. DiMitri, P. Emma, W. Fawley, K.-J. Kim, Z. Huang, C. Pellegrini, G. Penn, F. Sannibale, A. Sessler, G. Stupakov, J. Wurtele, M. Venturini, D. Xiang, M. Zolotorev.

REFERENCES

[1] Emma, P. *et al*., *Nature Photonics* **4,** 641–647 (2010).
[2] Ackermann, W. *et al*., *Nature Photonics* **1**, 336 (2007).
[3] Shintake, T. *et al.* , *Nature Photonics* **2,** 555–559 (2008).
[4] Altarelli, M. *et al.* (eds), "XFEL: The European X-ray free-electron laser technical design report", DESY 2006-097 (DESY, 2007).
[5] Shintake, T. *et al., Proc. 1st Int. Particle Accelerator Conf.* **TUXRA02,** 1285–1289 (2010).
[6] Patterson, B. D. *et al., New J. Phys.* **12**, 035012 (2010).
[7] Kim E.-S. and Yoon M., *IEEE T. Nucl. Sci.* **56,** 3597–3606 (2009).
[8] Faatz, B. *et al., Proc. 1st Int. Particle Accelerator Conf.* **TUPE005,** 2152–2154 (2010).
[9] https://slacportal.slac.stanford.edu/sites/lcls_public/lcls_ii/Pages/default.aspx.
[10] Kondratenko, A. and Saldin, E., *Part. Accelerators* **10**, 207-216 (1980).
[11] Bonifacio, R., Pellegrini, C. & Narducci, L., *Optics Commun*. **50,** 373–378 (1984).
[12] Barletta, W. *et al.* , *Nucl. Instr. and Methods in Phys. Res.* A **618**, 69–96 (2010).
[13] Madey, J., *Reviews of Acc. Sci. and Techn*. **3**, 1-12 (2010).
[14] Kim, K.-J., Sessler, A., *Science* **250**, 88-93 (1990).
[15] O'Shea, P. and Freund, H., *Science* **292**, 1853-1858 (2001).
[16] Pellegrini,C. and Stöhr, J., *Nucl. Instr. and Methods in Phys. Res.* A **500**, 33–43 (2003).
[17] M.-E. Couprie and J.-M. Filhol, C. R. Physique **9** (2008).
[18] McNeil, B. and Thompson, N., *Nature Photonics* **4**, 814-821(2007).
[19] See, for example, annual Proceedings of Free-Electron Laser conference accessible http://www.jacow.org/
[20] Csonka, P., *Part. Accelerators***11**, 45 (1980).
[21] Kincaid, B. *et al*., *AIP Conf. Proc.* **118,** 110 (1984).
[22] Bonifacio, R., de Salvo Souza, L., Pierini, P., Scharlemann, E. T., *Nucl. Inst. Meth. Phys. Res. A* **296,** 787–790 (1990).
[23] Yu L.-H. , *Phys. Rev. A* **44,** 5178–5193 (1991).
[24] Doyuran, A. *et al., Phys. Rev. Lett. 86*, 5902–5905 (2001).
[25] Murphy, J.B., Pellegrini, C., *Laser Handbook*, Elsiever, London, 9(1990).
[26] Yu L.-H. , *Phys. Rev. Lett.* **91,** 074801 (1991).
[27] Penco, G., *Proc. 1st Int. Particle Accelerator Conf.* **TUOARA02,** 1293–1295 (2010).
[28] Krausz, F., Ivanov, M., *Rev. Mod. Phys.* **81**, 163 (2009).
[29] Dromey, B. , *et al., Nat. Phys.* **2**, 456 (2006).
[30] Lambert, G., *et al*., *Nature Phys.* **4,** 296–300 (2008).
[31] Gullans, M., Penn, G., Zholents, A., *Opt. Commun*. **274**, 167 (2007).
[32] Stupakov, G., *Phys. Rev. Lett.* **102**, 074801 (2009).
[33] Xiang, D., Stupakov, G., *Phys. Rev. ST Accel. Beams* 12, 030702 (2009).
[34] Xiang, D. *et al. Phys. Rev. Lett*. **105,** 114801 (2010).
[35] Saldin, E. L., Schneidmiller, E. A. & Yurkov, M. V., *Opt. Commun.* **202,** 169–187 (2002).
[36] Feldhaus, J., *Optics Comm*. **140**, 341(1997).
[37] Shvyd'ko, Yu., "X-ray Optics", *Springer-Verlag New York, LLC*., (2004).
[38] Geloni, G., Kocharyan, V., Saldin, E., DESY 10-080(2010), arXiv:1006.2045v1
[39] Geloni, G., Kocharyan, V., Saldin, E., DESY 10-033(2010), arXiv:1003.2548v1
[40] Ding, Y., Huang, Z., Ruth, R. D., *Phys. Rev. Spec. Top. AB* **13,** 060703 (2010).
[41] See, for example, Brau, C. , "Free-Electron Lasers", *Academic*, San Diego, (1990).
[42] Colella, R. & Luccio, A., *Opt. Commun.* **50,** 41–44 (1984).
[43] Kim, K.-J., Shvyd'ko, Y. , Reiche, S., *Phys. Rev. Lett*. **100,** 244802 (2008).
[44] Kim, K.-J., Shvyd'ko, Y., *Phys. Rev. Spec. Top. AB* **12,** 030703 (2009).
[45] Shvyd'ko, Y. V. *et al.*, *Nature Phys.* **6,** 196–199 (2010).
[46] Lindberg, R. *et al*., in *Proc. FEL'09 Conf.*, **WEPC40,** Liverpool, UK, (2009).
[47] Vinogradov, A. V., Kozhevnikov, I. V., Popov, A. V., *Optics Comm*. **47**, 361(1983).
[48] Goldstein, J.C., McVey, B., Elliot, C.J., *Nucl. Instr. and Methods in Phys. Res.* A **272**, 177 (1988).
[49] Goldstein, J.C., McVey, B., Elliot, C.J., *Nucl. Instr. and Methods in Phys. Res.* A **296**, 288 (1990).
[50] Ciocci, F. *et al*., *IEEE J. Quantum Electr.* **31**, 1242 (1995).
[51] Dattoli, G., *et al*., *IEEE J. Quantum Electr*. **31** 1584 (1995).
[52] Attwood, D. T., "Soft X-Rays and Extreme Ultraviolet Radiation: Principles and Applications", *Cambridge Univ. Press*, Cambridge, (1999).
[53] Wurtele, J. *et al*., in *Proc. FEL'10 Conference*, Mälmo, Sweden, (2010).
[54] Zholents, A. , *Phys. Rev. ST Accel. Beams* **8**, 040701(2005).
[55] Ding, Y. *et al.* , *Phys. Rev. Lett.*, **102,** 254801 (2009).
[56] Zholents, A., *Reviews of Acc. Sci. and Tech*. **3**, (2010).
[57] Jones, D. *et al.*, , *Science* **288**, 635(2000).
[58] Baltuška, A. *et al*., *Nature* **421**, 611, 2003.
[59] Itatani, J., *Phys. Rev. Lett*. **88**, 173903(2002)

[60] Saldin, E.L, Schneidmiller, E.A., Yurkov, M.V., *Phys. Rev. ST Accel. Beams* **9**, 050702(2006).
[61] W.M. Fawley, *Nucl. Instr. and Methods in Phys. Res.* A **593,** 111(2008).
[62] Schweigert, I.V., Mukamel, S., *Phys. Rev. A* **76**, 012504 (2007).
[63] White paper: Scientific needs for future x-ray sources. *Publication ANL-08/39; BNL-81895; LBNL-1090E; SLAC-R-97*, (2008); http://www.als. publications/genpubs.html.
[64] Zholents, A., Penn, G., *Nucl. Instrum. Methods in Phys. Res. A* **612**, 254(2010).
[65] Geloni, G., Kocharyan, V., Saldin, E., DESY 10-006(2010), arXiv:1001.3506v1
[66] E. L. Saldin, E. A. Schneidmiller, and M.V. Yurkov, *Phys. Rev. ST Accel. Beams* **13**, 030701(2010).
[67] Wu, J., in *Proc. FEL'10 Conference*, Mälmo, Sweden, (2010).
[68] Loos, H., https://slacportal.slac.stanfor.edu/sites/ard_public/Pages /Announcements.aspx
[69] Zolotorev, M., *Nucl. Instrum. Methods in Phys. Res. A*, **483**, 445(2002).
[70] Gullans, M., Penn, G., Wurtele, J. S., Zolotorev, M., *Phys. Rev. ST Accel. Beams* **11**, 060701(2008).
[71] Prestemon, S. *et al., Proc. Particle Accel. Conf. 2009*, Vancouver, Canada, (2009).
[72] Eichner, T. *et al., Phys. Rev. ST Accel. Beams* **10**, 082401(2007).
[73] O'Shea, F. H. *et al., Phys. Rev. ST Accel. Beams* **13**, 070702(2010).
[74] Tanaka, T**.** *et al., New J. of Physics* **8**, 287(2006).
[75] Clarke, J. A., "The science and technology of undulators and wigglers", *Oxford University Press*, (2004).
[76] Emma, P. *et al., Proceedings of 2005 Part. Acc. Conf.*, Knoxville, USA, (2005).
[77] Reiche, S., Musumeci, P., Pellegrini, C., Rosenzweig, J. B., *Nucl. Inst. Meth. Phys. Res. A* **593,** 45–48 (2008).
[78] Hauri, C. P. *et al. , Phys. Rev. Lett.*, **104,** 2234802 (2010).
[79] Dowell, D., Schmerge, J., *Phys. Rev. ST Accel. Beams* **12**, 074201(2009).
[80] Dowell, D., *et al., Nucl. Instrum. Methods in Phys. Res. A*, (2010), doi:10.1016/j.nima.2010.03.104
[81] Baptiste, K., *et al., Nucl. Inst. Meth. in Phys. Res. A*, **599**, 9-14(2009).
[82] Baptiste, K., *et al.,* in *Proc. FEL'09 Conf.*, **WEOA05,** Liverpool, UK, (2009).
[83] Hunag, Z., *et al., Phys. Rev. ST Accel. Beams* **13**, 020703(2010).
[84] Akre, R., *et al.*, in *Proc. FEL'08 Conf.*, **FRAAU04,** Gyeongju, Korea, (2008).
[85] Emma, P., *SLAC-TN-05-004*, November 14, 2001.
[86] Gurevich, A. , *SRF Material Workshop*, FNAL, Batavia, IL, May 23-24, 2007.
[87] Pellin, M. J., Elam, J. W., Moore, J., *ECS Trans. 11(7, Atomic Layer Deposition Applications 3)*: 23-28 (2007).
[88] Zholents, A. *et al.*, in *Proc. Linac'08 Conf.*, **TUP046,** Victoria, Canada, (2008).
[89] Bartolini, R. *et al.*, in *Proc. FEL'09 Conf.*, **WEOB02,** Liverpool, UK, (2009).
[90] Loeh, F. *et al.*, in *Proc. 1st Int. Particle Accelerator Conf.* **MOZRA01,** Kyoto, Japan, (2010).
[91] Xiang, R. *et al.*, in *Proc. FEL'09 Conf.*, **WEOB04,** Liverpool, UK, (2009).
[92] Thomas, A. G. R. & Krushelnick, K., *Phys. Plasmas* **16,** 103103 (2009).
[93] Kneip, S. *et al., Phys. Rev. Lett*. **100,**105006 (2008).
[94] Gea-Banacloche, J. *et al., IEEE J of Quantum Electronics*, QE-23, No. 9. 1558(1987).
[95] Gea-Banacloche, J., Moore, G. T., Scully, M., *Proc. SPIE*, **453**, 393-401(1984).
[96] Dobiasch, P., Meystre, P., M. 0. Scully, *IEEE J. Quantum Electron.*, QE-19, 1812(1983).
[97] Bacci, A. *et al., Phys. Rev. ST Accel. Beams* **9**, 060704(2006).
[98] See, for example, Leemans, W., Esarey, E., *Physics Today*, **62**, 44-49(2009).